



Cite this: *Mater. Adv.*, 2025,  
6, 479

## Biomimetic haloperoxidases for antifouling on the surface of marine materials: a review

Meinan Yang,<sup>ab</sup> Nan Wang, <sup>\*ac</sup> Ruiyong Zhang, <sup>\*ac</sup> Sikandar Khan,<sup>ad</sup> Baorong Hou<sup>ac</sup> and Wolfgang Sand<sup>a</sup>

Biological fouling has led to many direct and indirect adverse effects on human life since ancient times. For decades, researchers have been trying to develop effective antifouling strategies to prevent biofouling by marine organisms. The toxicity of conventional antifouling agents toward nontarget organisms has led to their gradual banning all over the world. Therefore, researchers have begun to focus on biomimetic haloperoxidases based on the natural antifouling capability of some marine algae that can effectively prevent the attachment of microorganisms by self-secreting haloperoxidases. Biomimetic haloperoxidases exhibit high stability and have low cost, making them a good alternative to natural enzymes, and they perform well in both laboratory and natural marine conditions. This review mainly focuses on vanadium-based, cerium-based, molybdenum-based and other biomimetic haloperoxidases materials. Among them, vanadium-based materials mainly include  $V_2O_5$  and vanadium-based derivatives. Cerium-based materials mainly include  $CeO_2$ , heteroatoms (such as carbon, nitrogen and lanthanide) doping cerium oxide, cerium oxide composite and Ce-MOF. Molybdenum-based materials mainly include molybdenum single-atom and molybdenum-based composites. Other biomimetic haloperoxidase materials mainly include W-U<sub>i</sub>O and Cr-SA-CN semiconductors. Their efficient antifouling behavior and mechanisms have been highlighted. Certain shortcomings of biomimetic haloperoxidases and their prospects have also been described. Researchers are enthusiastic to exploit biomimetic haloperoxidases as efficient antifouling substances in marine environments.

Received 10th July 2024,  
Accepted 9th November 2024

DOI: 10.1039/d4ma00700j

[rsc.li/materials-advances](http://rsc.li/materials-advances)

## 1. Introduction

Scope and definition of biofilms vary depending on the field of research.<sup>1,2</sup> Most of the time, biofilms consist of a mixture of bacteria, fungi, protozoa, and/or algae that live in symbiosis with each other, and they are usually formed on moist surfaces, such as pipelines, cooling towers, drains, and other water delivery systems. Biofilms affect various industrial settings and production. Biofilms attached to ship hulls and seabed equipment traveling in the ocean are commonly called marine fouling.<sup>3</sup> Marine biofouling has many direct and indirect

effects on human life and activities. Marine fouling can contribute to surface deterioration of ships, damaging propellers, increasing resistance to forward movement and thereby resulting in more fuel consumption and excessive maintenance costs.<sup>4,5</sup> In addition, marine fouling indirectly contributes to global warming because excessive fuel consumption leads to more greenhouse gas emissions.<sup>6</sup> Besides, marine fouling leads to the collapse of the ecosystem due to biological invasion.<sup>7</sup> Some equipment for offshore operations has shown reduced capacity and safety due to the impact of marine fouling, such as subsea oil production and cross-sea bridges.<sup>8</sup> Therefore, it is particularly important to minimize or mitigate marine biofouling and reduce its huge financial impact.

Many measures have been taken to deal with marine fouling. Surface coating is the most widely used antifouling strategy in the marine industry. For example, traditional antifouling coatings consist of arsenic, zinc, tin and mercury to control marine fouling problems.<sup>9</sup> However, the impact of their toxicity on marine creatures cannot be ignored.<sup>10</sup> The International Maritime Organization decided to ban the use of biocides containing the aforementioned metals in the manufacture of antifouling coatings in 2003 and on the surface of ships in 2008.<sup>11</sup> Gradually,

<sup>a</sup> Key Laboratory of Advanced Marine Materials, Key Laboratory of Marine Environmental Corrosion and Bio-fouling, Institute of Oceanology, Chinese Academy of Sciences, Qingdao, 266071, China. E-mail: [wangnan123@qdio.ac.cn](mailto:wangnan123@qdio.ac.cn), [ruiyong.zhang@qdio.ac.cn](mailto:ruiyong.zhang@qdio.ac.cn)

<sup>b</sup> College of Marine Science and Biological Engineering, Qingdao University of Science and Technology, Qingdao, 266042, China

<sup>c</sup> Institute of Marine Corrosion Protection, Guangxi Key Laboratory of Marine Environmental Science, Guangxi Academy of Sciences, 98 Daling Road, Nanning 530007, P. R. China

<sup>d</sup> Department of Biotechnology, Shaheed Benazir Bhutto University, Sheringal, KP, 18000, Pakistan



these biofouling control measures were banned worldwide, and the search for safe, non-toxic, reliable and efficient antifouling measures began. So far, a number of green antifouling strategies and materials have been researched, such as novel functional polymers, micro-surface engineering, natural products and biomimetic materials.<sup>12</sup> Nature itself has plenty of ways to deal with the issue of biofilms attachment. Some compounds, such as terpenoids, steroids, carotenoids and capsaicin, are antifouling and can prevent biofouling.<sup>13</sup> In particular, vanadium-dependent haloperoxidase (VHPO) secreted by the marine algae (*Corallina officinalis* and *Delisea pulchra*) have been reported to prevent biofouling by catalyzing halides (Cl<sup>-</sup>, Br<sup>-</sup>) from seawater to hypohalous acids (HOBr, HOCl).<sup>14</sup> These hypohalous acids interfere with cell-to-cell communication (quorum sensing) of the bacteria by reacting with the signaling molecules of the marine bacteria, such as *N*-acyl homoserine lactones (AHLs). Thus, it is not easy for marine microorganisms to develop biofilms and adhere to surfaces.<sup>15</sup> But as natural enzymes, they have inevitable problems of high extraction/production costs, poor long-term stability, appropriate reaction conditions, *etc*. Therefore, it is the need of the day to develop biomimetic haloperoxidases with same or better enzyme catalytic performance and long-term stability in natural marine environment.

Many biomimetic haloperoxidases with excellent performance have been developed so far. In 1992, *cis*-dioxovanadium (VO<sup>2+</sup>) in acidic aqueous solution was the first reported vanadium bromoperoxidase biomimetic enzyme.<sup>16</sup> Natalio and his colleagues have developed vanadium pentoxide nanoparticles that mimic vanadium haloperoxidases, thwarting biofilm formation in 2012.<sup>17</sup> In addition to vanadium oxides, there are many vanadium-based complexes. A series of oxoperoxovanadium model complexes was characterized as the functional model for the vanadium haloperoxidase.<sup>18</sup> As observed in enzymes, the complexes have the reactivity of reproducing the peroxidative halogenation and halide-assisted peroxide disproportionation reactions. Due to the toxic effects of vanadium on the environment, subsequent research has gradually focused on green biomimetic enzymes. Herget and co-workers found that the oxides of cerium (CeO<sub>2-x</sub> nanorods) have the properties of quorum-sensing regulators, similar to natural vanadium haloperoxidases (V-HPOs).<sup>14</sup> Wu *et al.* used a room-temperature synthesis method to obtain a new morphology of CeO<sub>2</sub> rich in oxygen vacancies.<sup>19</sup> Wang and her colleagues synthesized nitrogen-doped CeO<sub>2</sub> with a core-shell structure using a simple coprecipitation method.<sup>20</sup> Certain carbon-nitrogen and lanthanide-doped cerium oxide have also been developed.<sup>21,22</sup> In addition to single atoms, cerium oxide can also be combined with other metal oxides such as zirconia.<sup>23</sup> The emergence of these derivatives can help reduce the amount of cerium atoms, while maintaining or even improving the performance of the catalyst. Molybdenum-based biomimetic enzymes and their derivatives have also become a focus of attention, such as molybdenum single-atom and Co-MoS<sub>2</sub>.<sup>24,25</sup> Some metal nanoparticles also have an antimicrobial effect.<sup>26,27</sup> Therefore, this review focuses on biomimetic haloperoxidases, their antifouling efficacy and mechanism of fouling inhibition.

## 2. Vanadium-based biomimetic enzyme

Inspired by the natural vanadium haloperoxidase produced by certain marine algae, which prevents the colonization of certain fouling causing marine organisms and seaweeds, the functional recombinant VHPO was manufactured.<sup>28</sup> Although the effect of functional recombinant VHPO is better than VHPO itself, some issues still need to be addressed. For instance, the production costs of additives used in antifouling coatings is higher in mass production. There are problems with its stability and reactivity in seawater conditions. Therefore, it is necessary to find suitable enzyme analogues as catalysts to replace VHPO. Researchers have gradually started their research on vanadium-based materials. For example, De la Rosa *et al.* reported the first vanadium bromoperoxidase biomimetic enzyme VO<sup>2+</sup> in acidic aqueous solution.<sup>16</sup> Butler and his co-workers found ammonium metavanadate (NH<sub>4</sub>VO<sub>3</sub>), a functional mimic of vanadium-dependent bromoperoxidase (VBPO) in 1992 (Fig. 1(a)).<sup>16,29</sup> They successfully discovered that NH<sub>4</sub>VO<sub>3</sub> can catalyze the oxidative bromination of 3,3',5,5'-tetramethylbenzidine with KBr and H<sub>2</sub>O<sub>2</sub> under acidic condition (>0.001 M H<sup>+</sup>). Melissa and others found a six-coordinate vanadium complex (LVO(OEt)-(EtOH)), which can catalyze the oxidative bromination by hydrogen peroxide in DMF solution as the catalyst precursor (Fig. 1(b)–(e)).<sup>30</sup> In addition, Eshita and co-workers synthesized two new substances vanadium(IV) dioxide and vanadium(V) oxido-peroxido and confirmed that they have bioinspired catalytic activities.<sup>31</sup> The bromoperoxidase activities of these complexes are determined by activating the C–H bonds (such as phenol, o-cresol and p-cresol). Mannar and colleagues have synthesized one dioxido-vanadium(V) complex using 1-(2-pyridylazo)-2-naphthol donor ligand and grafted the complex through coordination of an imidazole-functionalized chloromethylated polystyrene (cross-linked with 5% divinylbenzene) (Fig. 1(f)).<sup>32</sup> It has been reported that these complexes exhibit catalytic activity as functional mimics of oxidative bromination of organic substrates.

### 2.1. V<sub>2</sub>O<sub>5</sub>

Natalio and coworkers demonstrated that vanadium pentoxide (V<sub>2</sub>O<sub>5</sub>) nanowires have peroxidase-like activity.<sup>17</sup> V<sub>2</sub>O<sub>5</sub> nanowires are widely used as catalyst materials that are stable, cheap and easily available.<sup>33</sup> In the experimental conditions and the presence of H<sub>2</sub>O<sub>2</sub> and Br<sup>-</sup>, V<sub>2</sub>O<sub>5</sub> nanowires exhibit intrinsic bromination activity similar to natural enzymes (VHPO), producing HOBr acid with bactericidal effects (Fig. 2a). Also, the bactericidal performance does not weaken in the marine/field test. The test plate, which contains V<sub>2</sub>O<sub>5</sub> nanowires coating after 60 days of exposure to seawater, showed no biofouling on its surface, indicating that V<sub>2</sub>O<sub>5</sub> nanowires can effectively prevent biological fouling. This biomimetic method is stable, water-insoluble, slightly toxic and inexpensive. It replaces traditional chemical biocides with a new antibacterial, antifouling and disinfection formula.

### 2.2. Vanadium-based derivatives

To study biomimetic catalysts, researchers could start from the natural compound itself and adjust it on the basis of the



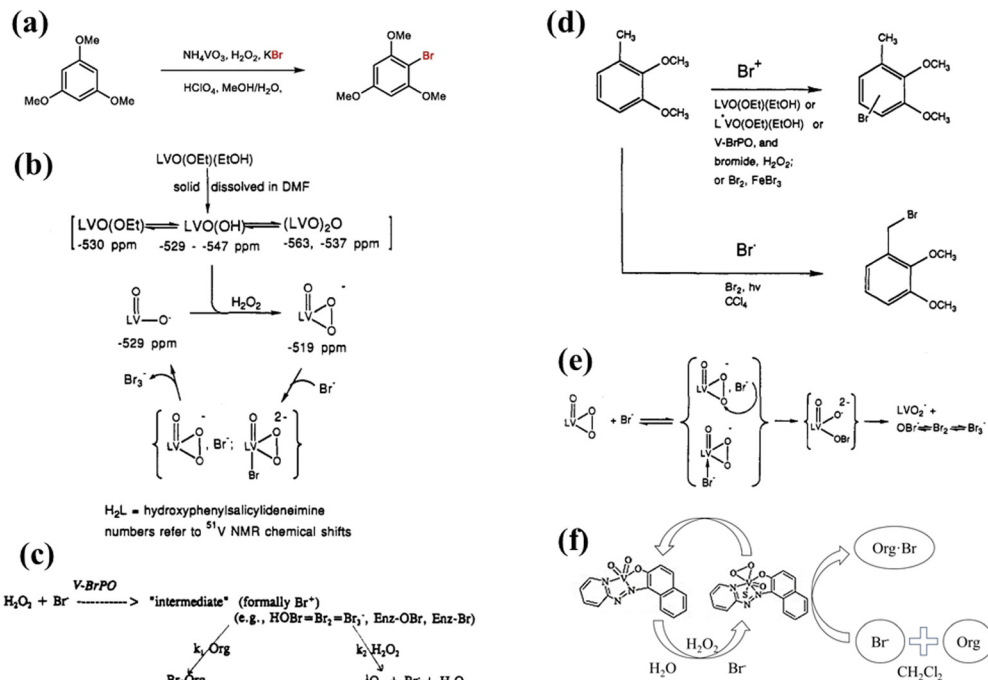


**Fig. 1** (a) Reaction equation of  $\text{NH}_4\text{VO}_3$ .<sup>29</sup> Reproduced from ref. 29 with permission from Elsevier, copyright 2022. (b)–(e) Four possible reaction mechanisms of  $\text{LVO(OEt)(EtOH)}$ .<sup>30</sup> Reproduced from ref. 30 with permission from ACS, copyright 1993. (f) Reaction diagram of a tridentate oxygen–nitrogen–nitrogen donor ligand, 1-(2-pyridylazo)-2-naphthol.<sup>32</sup> Reproduced from ref. 32 with permission from Elsevier, copyright 2014.

original to obtain a better simulant.<sup>34</sup> VHPO is naturally present in some algae and fungi, and due to its catalytic activity and defense mechanism against microorganisms (Fig. 2b–d),<sup>18</sup> it has aroused the interest of researchers. By mimicking the structure and function of VHPO in the form of reactive

peroxides, researchers have designed different metal–organic compounds. Colpas and colleagues produced a series of oxo-peroxovanadium complexes, which have the ligands  $\text{H}_3\text{nta}$  = nitrilotriacetic acid,  $\text{H}_3\text{heida}$  = *N*-(2-hydroxyethyl)iminodiacetic acid,  $\text{H}_2\text{ada}$  = *N*-(2-amidomethyl)iminodiacetic acid,

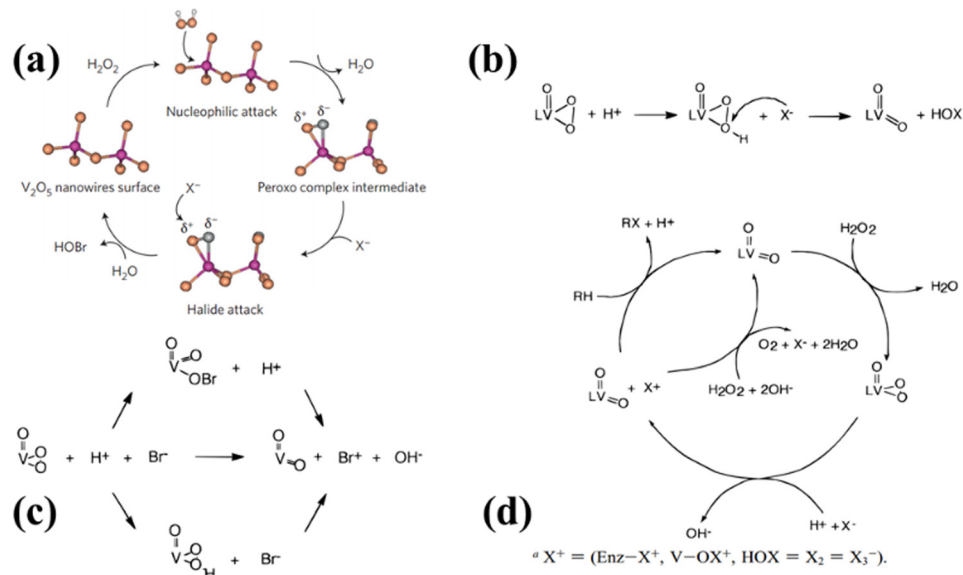


**Fig. 2** (a) Catalytic bromination mechanism for  $\text{V}_2\text{O}_5$  nanowires.<sup>17</sup> Reproduced from ref. 17 with permission from Springer Nature, copyright 2012. (b), (c) and (d) are several possible mechanisms of halide oxidation in the vanadium haloperoxidase functional model.<sup>18</sup> Reproduced from ref. 18 with permission from ACS, copyright 1996. (b) Halide oxidation reaction mechanism involves the nucleophilic attack of halides on the protonated peroxide ligand of the complex, resulting in oxygen transfer and simultaneous two-electron transfer. (c) The limiting forms for the potential mechanistic pathways. (d) Catalytic cycle of the vanadium haloperoxidase enzyme.

$\text{Hbpg} = N,N\text{-bis}(2\text{-pyridylmethyl})\text{-glycine}$ , and  $\text{tpa} = N,N,N\text{-tris}(2\text{-pyridylmethyl})\text{amine}$  and were characterized as functional models of vanadium peroxidase.<sup>18</sup> These complexes contain the crystal structures of  $\text{K}[\text{VO}(\text{O}_2)\text{Hheida}]$ ,  $\text{K}[\text{VO}(\text{O}_2)\text{ada}]$ ,  $[\text{VO}(\text{O}_2)\text{bpg}]$ , and  $\text{H}[\text{VO}(\text{O}_2)\text{bpg}]_2(\text{ClO}_4)$ . They were designed after getting inspired by the structure of VHPO, namely, recombinant functional enzymes. These complexes were verified to have the ability of catalyzing peroxidative halogenation reaction with the support of experimental data.<sup>18</sup> VHPOs have the umbrella-type vanadium peroxy-oxo structure that is a valid model in the vanadium oxide biocatalyst system as do mimics compounds, for example,  $\text{K}[\text{VO}(\text{O}_2)\text{Hheida}]$ .

Although vanadium-based materials have excellent antifouling effect, its large-scale applications could be limited because of the mutagenic, carcinogenic and teratogenic of vanadium compounds.<sup>14</sup> Since a great deal of environmental issues exist with the use of the heavy metal vanadium, an antifouling metal with high biocompatibility would be highly advantageous.

### 3. Cerium-based biomimetic enzymes

Following the catalytic activity of oxidation/halogenation reaction,<sup>35</sup> the oxyhalogenation of activated arenes,<sup>36</sup> and role of the  $\text{Ce}^{3+}/\text{Ce}^{4+}$  redox couple in the halogenation of malonic acid in the Belousov-Zabotinsky reaction,<sup>37</sup> Karoline Herget deeply investigated the intrinsic haloperoxidase activity of ceria nanoparticles on anti-biological antifouling.<sup>14</sup>

#### 3.1. $\text{CeO}_2$

Cerium can be reversibly converted between trivalent and tetravalent states by the redox potential of  $\text{Ce}^{3+}/\text{Ce}^{4+}$ .  $\text{CeO}_2$  is an excellent oxide in the industry because it has oxygen vacancy defects. These defects can be quickly filled and discharged, which makes  $\text{CeO}_2$  a high oxygen storage compound.<sup>38</sup> For example, Deshpande *et al.* showed that  $\text{CeO}_2$  nanoparticles could form more oxygen vacancies as the particle size decreases to improve its activity and exhibit catalytic properties.<sup>39</sup> In addition, the valence states of cerium in cerium oxide and cerium oxides' defect structure are dynamic and affected by physical factors (such as reaction temperature, time and other ions).<sup>40</sup> Tremel's group showed that synthesis time could directly control the surface properties of mesoporous ceria

and the chemical activity of  $\text{CeO}_{2-x}$  nanoparticles in haloperoxidase- and peroxidase-like reactions scales with their surface defects (*via* the  $\text{Ce}^{3+}/\text{Ce}^{4+}$  ratio).<sup>41</sup>

Herget *et al.* clearly showed that  $\text{CeO}_{2-x}$  nanorods embody intrinsic haloperoxidase-like activity because  $\text{CeO}_{2-x}$  nanorods could successfully catalyze organic signaling compounds and cause them to undergo a bromination reaction.<sup>14</sup> Test plates are daubed with the coatings, self-polishing resin formulation (SF) used for boat hull and hard paint formulations (HF), which contained experimentally synthesized  $\text{CeO}_{2-x}$  nanorods. In static field tests, the plates illustrated favorable nanoparticle enzyme mimic property, upsetting surface seaweed colonization (Fig. 3a). Under many environments, biofouling could significantly reduce the usage life of polymer nanofibers. Biofouling, especially biofilm contaminations, adheres to the surface by microbiological nonspecific adhesion.<sup>42</sup> The adhesion layer that exists in nanofibrous surface is difficult or even impossible to remove. Hu's team synthesized  $\text{CeO}_{2-x}$  nanorods and used them to electrospin with polyvinyl alcohol (PVA) to create freestanding nanofiber pads.<sup>43</sup> Synthetic mechanically sturdy mixing pads can catalyze the oxidation of  $\text{Br}^-$  and  $\text{H}_2\text{O}_2$  to  $\text{HOBr}$  because the cerium compound has similar activity to natural halogenated peroxidase. The destruction of quorum sensing effect by  $\text{HOBr}$  prevents the formation of biofilms on the surface of the fiber pad (Fig. 3b).

Due to the widespread applications of  $\text{CeO}_2$  nanoparticles, it is urgent for humans to fully understand the ecotoxicological effects of nanoceria oxide on human health and environment. Some reports showed that  $\text{CeO}_2$  nanomaterials have negative impacts on organisms at very low concentrations.<sup>44</sup> The toxicity of different morphologies and doped materials of nanoceria are further needed to be investigated.

#### 3.2. Heteroatoms-doped cerium oxide

Cerium oxides have excellent catalytic activity as haloperoxidase mimics. As a rare earth metal, cerium is very difficult to extract although its chemical elements are stored in abundant quantities on the earth. They are usually formed into alloys in pairs, which need to be separated. These rare-earth elements are relatively dispersed in the earth's crust and there are few mineral deposits with high abundance. This feature limits its large-scale application. Doping with other elements in cerium

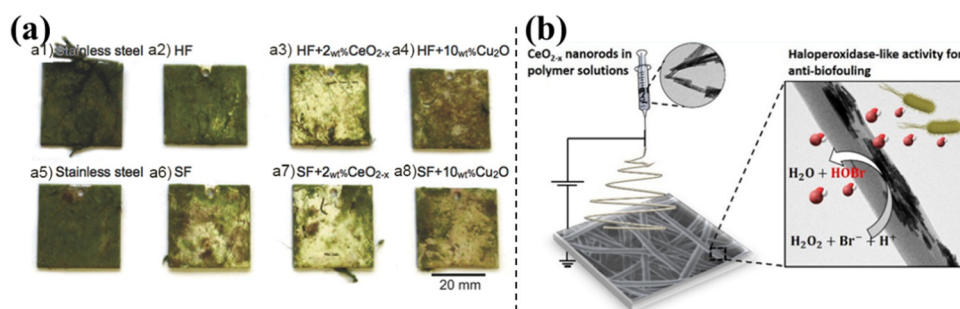


Fig. 3 (a) Selected samples after seven and half weeks of the static field immersion.<sup>14</sup> Reproduced from ref. 14 with permission from Wiley, copyright 2017. (b) Fabrication of  $\text{CeO}_{2-x}$  nanofibrous mats by electrospinning.<sup>43</sup> Reproduced from ref. 43 with permission from ACS, copyright 2018.



oxide is an efficient measure to decrease the consumption of cerium.

**3.2.1. Carbon-doped cerium oxide.** Carbon-based materials have demonstrated the ability of enzyme mimics. Shi *et al.*<sup>45</sup> found that carbon nanodots possess intrinsic peroxidase-like activity and can produce chromogenic reactions by the  $\text{H}_2\text{O}_2$ -catalyzed oxidation of 3,3',5,5'-tetramethylbenzidine. Carbon-based materials show great prospects as substitutes for similar enzyme catalysts because of their rich reserves, adjustability and high stability.<sup>20,46</sup> Hence, it is a valid strategy to improve the catalytic activity and reduce the use of rare metals by carbon doping. Using carbon spheres as a template, the core-shell structure of carbon was prepared by a simple coprecipitation method. Wang and co-workers successfully synthesized  $\text{CeO}_2@C$  using this approach.<sup>20</sup> Prior to field experiments, phenol red (PR) was used to test whether the material had the required catalytic properties and excellent performance (Fig. 4a). Due to carbon doping, the performance and stability of  $\text{CeO}_2@C$  was improved. As shown in Fig. 4b, there is a sharp and prominent peak at 590 nm, illustrating that  $\text{CeO}_2@C$  equally has good intrinsic haloperoxidase mimicking activity. Through the comparison of experimental results of  $\text{CeO}_2$  and  $\text{CeO}_2@C$ , it is obvious that the catalytic activity of the same amount carbon-doped  $\text{CeO}_2$  is higher than that of  $\text{CeO}_2$ . Antimicrobial performance analysis was done in the presence of substrates  $\text{H}_2\text{O}_2$  and  $\text{Br}^-$ , and experimental titanium plate containing  $\text{CeO}_2@C$  was shown to be completely black (Fig. 4c). It illustrates that the surface of this titanium plate is free of bacterial adhesion, which was in stark contrast to the dense bacterial population on the  $\text{CeO}_2@C$ -free group (blank). These results indicated that  $\text{CeO}_2@C$  possesses significant

bromination activity and could catalyze the oxidation of  $\text{Br}^-$  by  $\text{H}_2\text{O}_2$  to generate the relevant  $\text{HOBr}$ , which shows antibacterial activity. Compared to  $\text{CeO}_2$ , the  $\text{CeO}_2@C$  composite reduces the usage of rare-earth metal cerium during the synthesis process and measurably enhances the catalytic activity. This work provides a new method and research direction for antimicrobial, antifouling and disinfection.

**3.2.2. Nitrogen-doped cerium oxide.** Compared to carbon-doped cerium oxide, nitrogen doping is also a better option. Wang *et al.* synthesized nitrogen- and carbon-doped  $\text{CeO}_2$  (N-C/ $\text{CeO}_2$ ) using a combination of liquid and solid.<sup>21</sup> The product has halogenated peroxidase activity over a wide temperature range (20–50 °C), with simultaneously high catalytic stability/recyclability (Fig. 4c). Unlike the synthetic method of other studies,<sup>20,47</sup> N-C/ $\text{CeO}_2$  only uses melamine to provide a combined nitrogen and carbon source. Coupled with the synthesis methods of liquid and solid phase, it makes synthesis easier. There is one defect of existing unknown parts in the formation mechanism of N-C/ $\text{CeO}_2$ , which need to be further improved because its catalytic activity is mainly derived from  $\text{CeO}_2$ . Generally, this work offers a haloperoxidase mimic that is an efficient, novel and sustainable antimicrobial material.

**3.2.3. Lanthanide-doped cerium oxide.** The defects of ceria are closely related to its catalytic performance. The metal related to oxygen vacancies is able to substitute these defects<sup>48</sup> using metal dopants. The mechanochemical synthesis method is different compared to our normal hydrothermal synthesis. The mechanochemical synthesis of oxide is accomplished by an external mechanical force such as high-energy ball milling or grinding<sup>49</sup> using chlorides of lanthanides as starting compounds

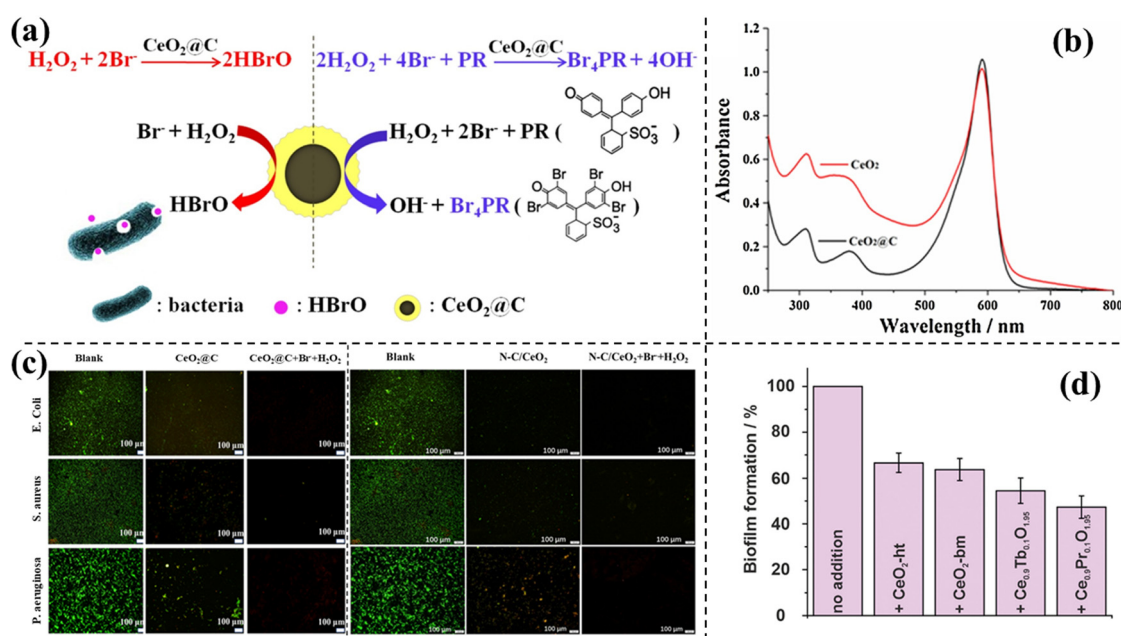


Fig. 4 (a) Reaction mechanism of  $\text{CeO}_2@C$  as a haloperoxidase mimic.<sup>20</sup> Reproduced from ref. 20 with permission from Elsevier, copyright 2020. (b) Absorbance spectra of solutions catalyzed by  $\text{CeO}_2@C$  and  $\text{CeO}_2$  HS.<sup>20</sup> Reproduced from ref. 20 with permission from Elsevier, copyright 2020. (c) Live/dead staining images of *E. coli*, *S. aureus* and *P. aeruginosa*.<sup>20,21</sup> Reproduced from ref. 20,21 with permission from Elsevier and MDPI, copyright 2020 and 2023. (d) Crystal violet staining assay of *P. aeruginosa* grown in lysogeny broth.<sup>22</sup> Reproduced from ref. 22 with permission from RSC, copyright 2022.



and then the doped activated ceria that has a non-balanced structure. Opitz *et al.* selected elements of the lanthanide series, such as europium (Eu), dysprosium (Dy), gadolinium (Gd) and samarium (Sm) and doped them in nanoceria<sup>22</sup> to investigate if they could enhance the catalytic activity of halogenated peroxide reactions. Some of them showed enhancement of catalytic activity, while others had less effect. They selected four materials for the detailed study:

- (i) Pure, undoped ceria.
- (ii) Tb-doped ceria with moderate catalytic activity as a doped representative.
- (iii) Pr-doped ceria with the highest catalytic activity as a representative.
- (iv)  $\text{Ce}_{1-x}\text{Ln}_x\text{O}_{2-x/2}$  nanocrystal prepared by hydrothermal synthesis as a comparison of the balance structure.

From (i) to (iii), the mechanochemical synthesis method is used. Lanthanide metals can be incorporated into the body of ceria by this synthesis method without solubility limitations. Agglomeration influences the formation of nanoceria, but sodium chloride, a by-product of mechanochemical metathesis reaction, inhibits agglomeration by matrix effects. In subsequent experiments, some verdicts are shown and are reasonable to explain the enhancement of catalytic activity. As confirmed by ESR spectroscopy, doping  $\text{Pr}^{3+}$  and  $\text{Tb}^{3+}$  by ball-milling synthesis increases the oxygen defect of surface sites. This means that these dopants stabilize  $\text{O}_2^-$  radicals, which are important for catalysis. Dopants bring high defect density and positive surface point, which might be the cause of the high catalytic performance. According to the crystal violet staining assay, the number of adherent *P. aeruginosa* cells is in the order  $\text{CeO}_2$  (ht) >  $\text{CeO}_2$  (bm) >  $\text{Ce}_{0.9}\text{Tb}_{0.1}\text{O}_{1.95}$  >  $\text{Ce}_{0.9}\text{Pr}_{0.1}\text{O}_{1.95}$  (ht: hydrothermal, bm: ball milled) (Fig. 4d). Contrary to pure  $\text{CeO}_2$  and blank surface,  $\text{Ce}_{0.9}\text{Pr}_{0.1}\text{O}_{1.95}$  demonstrates an obvious reduction of biofilm formation.

Through a series of experiments, Phil Opitz demonstrated that the halogenated activity of  $\text{CeO}_2$  can be reinforced by substituting  $\text{Ce}^{4+}$  with  $\text{Ln}^{3+}$  in  $\text{Ce}_{1-x}\text{Ln}_x\text{O}_{2-x/2}$ . Also, mechanochemical synthesis could accomplish energy saving in large industrial quantities and the production of residue-free Ln-doped nanoceria. Bionic method replaces the traditional bactericide and expensive enzyme preservation system with steady, nontoxic and abundant rare-earth oxides. This is an important step towards a sustainable solution to the problem of antifouling.

### 3.3. Cerium oxide composite

Ultra-small nanoclusters on different supports will show coalescence and agglomeration, which will lead to the loss of their catalytic activity.<sup>50</sup> Luo *et al.* proposed a way to make hybrid  $\text{CeO}_2@\text{ZrO}_2$  (Fig. 5a).<sup>23</sup> These ceria clusters have high density and ultra-small ( $\approx 0.8$  nm) size, which are steadied on the  $\text{ZrO}_2$  substrates. This unique feature of heterografted  $\text{CeO}_2@\text{ZrO}_2$  nanozymes resulted in excellent and stable halo-peroxidase mimicking performance in selectively catalyzing the oxidation of  $\text{Br}^-$  to  $\text{HOBr}$  by  $\text{H}_2\text{O}_2$ . Its performance is much better than that of the original  $\text{CeO}_2$  nanoparticles. By producing bactericidal hypobromous acid,  $\text{CeO}_2@\text{ZrO}_2$  can effectively combat the colonization of antibiotic-resistant bacteria. Not only in lab experiments,  $\text{CeO}_2@\text{ZrO}_2$  shows excellent antibacterial activity in the presence of  $\text{Br}^-$  and  $\text{H}_2\text{O}_2$  (Fig. 5b) and also in field (marine environments), illustrating good results. As a surface-coating additive,  $\text{CeO}_2@\text{ZrO}_2$  added to the test plates significantly prevented marine biofilm colonization. It is important that this work emphasizes the role of reasonable design and synthesis in improving the nanozyme performance and provides a new insight into the design of highly-active catalytic nanomaterials for various antibacterial applications.

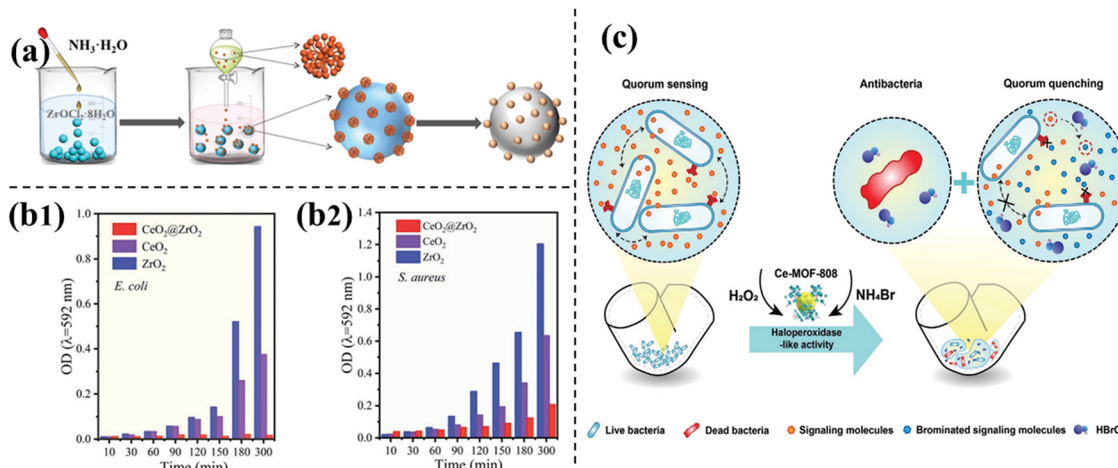


Fig. 5 (a) Schematic of the synthetic process of  $\text{CeO}_2@\text{ZrO}_2$ .<sup>23</sup> Reproduced from ref. 23 with permission from Wiley, copyright 2022. (b) Antibacterial and antibiofouling capacity of  $\text{CeO}_2@\text{ZrO}_2$ . Growth behavior of (b1) *E. coli* and (b2) *S. aureus* after coincubation with different combinations.<sup>23</sup> Reproduced from ref. 23 with permission from Wiley, copyright 2022. (c) Schematic of Ce-MOF-808 for antibacterial activity and inhibiting the formation of biofilms based on its HPO-like activity.<sup>51</sup> Reproduced from ref. 51 with permission from Wiley, copyright 2022.



### 3.4. Ce-MOF

During the last decade, metal-organic frameworks (MOFs) have become one of the most promising catalyst materials. The reason is that MOFs have a large surface area, high porosity, homogeneous structure, molecular/atom-level catalytic centers and so on.<sup>52</sup> The easily doped heteroatoms in MOFs provide a good opportunity for the synthesis of catalysts with excellent performance. The special structure of MOF, ultra-high surface area<sup>53</sup> and numerous substrate-binding reaction sites<sup>54</sup> are conducive to the binding of cerium ions, and the great prospect of assembling multiple active sites make it an excellent choice. Zhou and *et al.* selected MOF with the different nature of the materials used (Fig. 5c).<sup>51</sup> The MOF in this work has primary and secondary coordination environments similar to natural enzymes<sup>55</sup> and is an ideal enzyme-like mimic.<sup>56</sup> The synthetic biomimetic material were named as Ce-MOF-808. MOF-808 is one of the MOFs, its framework contains H<sub>3</sub>BTC as a ligand. According to BET analysis, the good surface area may expose multiple active sites, thereby promoting the good catalytic activity of MOFs, which in turn produces good biofilm inhibition capacity. Although the antibacterial effect of Ce-MOF-808 is not as good as V<sub>2</sub>O<sub>5</sub> nanowires, Ce-MOF-808 is another potential antifouling option due to its activity of HPO-like inhibition of bacterial growth. Ce-MOF-808 is easy to prepare, and its HPO-like activity could catalyze the oxidative bromination of bacterial quorum sensing (QS) signal molecule AHLs. This response achieves the effect of quorum quenching (QQ), thereby preventing biofilm formation and growth. In pipes, they build a pipe-adhered biofilm model. Hence, in the presence of Br<sup>-</sup> and H<sub>2</sub>O<sub>2</sub>, Ce-MOF-808 plays an efficient role in restraining surface-adhered biofilm formation. These findings make it useful for water pipe cleaning. In addition to excellent enzyme-like activity, Ce-MOF-808 also has better performance in terms of long-stability, recyclability and biosecurity.

The discovery of Ce-MOF-808 enlarges the finite scope of HPO-like mimics and promotes the substitution of natural HPO to prevent the formation of biofilm attached to the interior of the pipeline. Moreover, it offers extensive antifouling application possibilities on multiple material surfaces.

## 4. Molybdenum-based biomimetic enzymes

### 4.1. Molybdenum single-atom

For general nanozymes, it is important to compare the number of active sites in nanozymes with corresponding enzymes.<sup>57</sup> However, only a small number of active atoms on the surface contribute to the enzyme-like catalysis. Consequently, this leads to a low density of active sites, poor atom utilization efficiency, and reduced catalytic activity.<sup>58</sup> Therefore, single atom becomes the site of focus for many researchers. As catalysis materials, single atoms have the advantage of atomic dispersion active sites,<sup>58,59</sup> high utilization, high activity and high selectivity,<sup>60</sup> which can be good substitutes. According to the Arrhenius equation, chemical reactions are directly proportional to temperature.<sup>61</sup> The thermal effect of sunlight is a non-invasive external stimulus, and this thermal effect can be considered to enhance the activity of HPO-like nanozymes. Wang and co-workers explored a single atom molybdenum nanozyme (Mo SA-N/C) with the photothermal effect to prevent biofouling.<sup>24</sup> As a result of Mo doping, the nanomaterials possess intrinsic HPO-like activity that could catalyze the oxidation of Br<sup>-</sup> and H<sub>2</sub>O<sub>2</sub> to produce HOBr. Under visible light irradiation, the photothermal effect of Mo SA-N/C enhances HPO-like activity. It is evident that the antibacterial effect under light conditions is about twice that of under dark conditions (Fig. 6a). This study offered a new idea for the efficient and eco-friendly preparation of antifouling materials.

### 4.2. Molybdenum-based composites

MoS<sub>2</sub> itself has a certain haloperoxidase activity. On doping Co transition metal in MoS<sub>2</sub>,<sup>25</sup> the new biomimetic enzyme has good halogenated peroxidase activity, which can catalyze the oxidation of Br<sup>-</sup> to HOBr (Fig. 6b). It is about 2 times higher than that of Ni-doped MoS<sub>2</sub> and about 23 times higher than that of undoped MoS<sub>2</sub>. EPR analysis proves that the increase in the activity is attributed to changes in the sulfur vacancy concentrations. The sulfur vacancy concentration of Co-MoS<sub>2</sub> is evidently higher than that of Ni-MoS<sub>2</sub> and pure MoS<sub>2</sub> (Fig. 6c). The stability, antibacterial performance and yield of Co-MoS<sub>2</sub> in

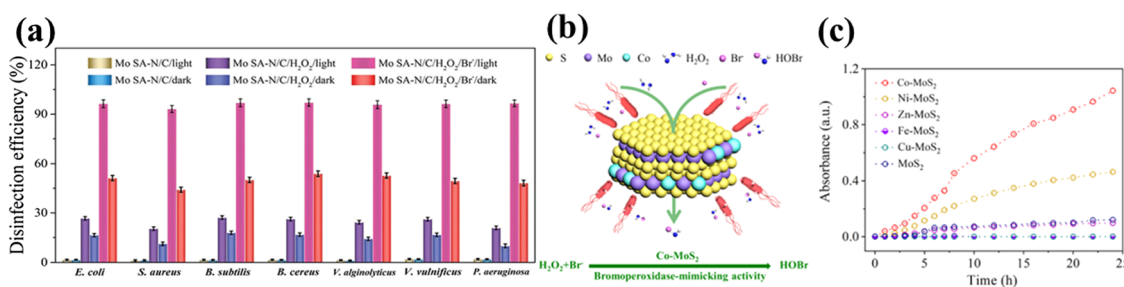


Fig. 6 (a) Disinfection efficiency of Mo SA-N/C, Mo SA-N/C + H<sub>2</sub>O<sub>2</sub>, and Mo SA-N/C + Br<sup>-</sup> + H<sub>2</sub>O<sub>2</sub> under dark or visible light illumination.<sup>24</sup> Reproduced from ref. 24 with permission from Wiley, copyright 2022. (b) Schematic of structure and reaction mechanism of the Co-MoS<sub>2</sub> nanozyme.<sup>25</sup> Reproduced from ref. 25 with permission from ACS, copyright 2022. (c) Time-dependent absorbance variation of phenol red solution at 590 nm with the use of different transition metal-doped MoS<sub>2</sub> nanozymes.<sup>25</sup> Reproduced from ref. 25 with permission from ACS, copyright 2022.



marine water show good performance, similar to that of the HPO-like mimic. One drawback is that it depends on the pH of the water environment. Compared to pH 5.7, the activity at pH 8.0 is 52%. The reduction may be related to the decrease of reactant activity and the decrease of the stability of HOBr and other reaction intermediates.

MoS<sub>2</sub> nanozyme was one of the primary attempts of transition metal engineering as functional mimics of natural halo-peroxidases in anti-biofouling research. The HPO-like activity is effectively enhanced by doping Co and produces a significant antibacterial role to *E. coli*, *S. aureus* and biofilm colonization in seawater. This study opens a new potential application of transition metal disulfides for combating biofouling.

MoS<sub>2</sub> is a kind of inorganic two-dimensional material. Except the haloperoxidase mimics, it has many other applications, such as energy, electronic, biosensor and immobilizing DNA strands after functionalization.<sup>62</sup> Therefore, the biological safety of molybdenum-based materials has become a problem worthy of attention. Studies have showed that there was a strong connection between well-exfoliated MoS<sub>2</sub> nanosheets and their cytotoxic behavior. Their toxicity was decreased by selecting the catalyst concentration.<sup>63</sup> However, so far, there is no absolute statement on the toxicity of MoS<sub>2</sub>.

## 5. Others biomimetic enzymes

### 5.1. W-UiO nanozyme

For nuclear power plants, uranium (U) is an essential element. Thus, the extraction of uranium is equally important.<sup>64</sup> Oceans contain approximately 4 billion tons of uranium resources, which equates to an inexhaustible supply for nuclear power production.<sup>65</sup> Uranium adsorbent is one of the strategies that have been used to extract U from marine resources. Metal-organic framework is a special porous hybrid material using metal ions and organic ligands,<sup>66</sup> which has a large surface area, high selectivity and good chemical stability.<sup>67</sup> Therefore, metal-organic frameworks are a good adsorbent for uranium extraction. However, it needs to stay in seawater for a long time so it also comes in contact with marine organisms causing

marine fouling. Furthermore, the performance of uranium adsorbent would gradually weaken.<sup>68</sup> Wang and co-workers gave a strategy for anchoring tungsten single atom for atomic engineering in a metal-organic framework.<sup>69</sup> This W-UiO nanozyme has intrinsic HPO-like activity, which can catalyze bromine ions into HOBr, which has a bactericidal effect (Fig. 7a). Consequently, it can improve the impact of adsorption performance from marine microbial colonization. After five regeneration cycles in natural seawater, the performance of W-UiO still remains 78% compared to that of unused W-UiO.

This provides a new idea to design recyclable, highly stable sorbents for extracting uranium from seawater. We can consider designing and manufacturing them to mimic the defenses of natural organisms.

### 5.2. Cr-SA-CN semiconductor nanozyme

The use of HPO-like nanozymes instead of natural enzymes to prevent biofouling in oceans is a widely adopted measure.<sup>14,17</sup> Haloperoxidase-catalyzed oxidation reactions require the involvement of H<sub>2</sub>O<sub>2</sub>, but in a normal marine water environment, the content of H<sub>2</sub>O<sub>2</sub> is very low. The upper layer of oceans generally contain H<sub>2</sub>O<sub>2</sub> at a concentration of about 102 nmol L<sup>-1</sup>.<sup>71</sup> The lower content of H<sub>2</sub>O<sub>2</sub> is a major obstacle to the complete production of hypohalogenic acid by HPO-like mimics. Because of this, building one generation system of H<sub>2</sub>O<sub>2</sub> is a good strategy. Luo and *et al.* constructed a semiconductor nanozyme that is composed of Cr single atoms coordinated on CN.<sup>70</sup> This is a dual functional nanozyme that has non-sacrificial H<sub>2</sub>O<sub>2</sub> photosynthesis and HPO-like activity. It uses water and O<sub>2</sub> to produce H<sub>2</sub>O<sub>2</sub> under visible light, thereby self-supplying H<sub>2</sub>O<sub>2</sub> in a continuous manner for HPO-like reactions (Fig. 7b). In actual field tests in seawater, the experimental results show that Cr-SA-CN can form an inert surface on the outer layer of the material when added to the coating as an antimicrobial agent, thereby preventing the colonization of marine microorganisms.

This work proves the potential of single atom nanozymes in combating biofouling and also promotes the development of multifunctional nanozymes for biomimetic antifouling.

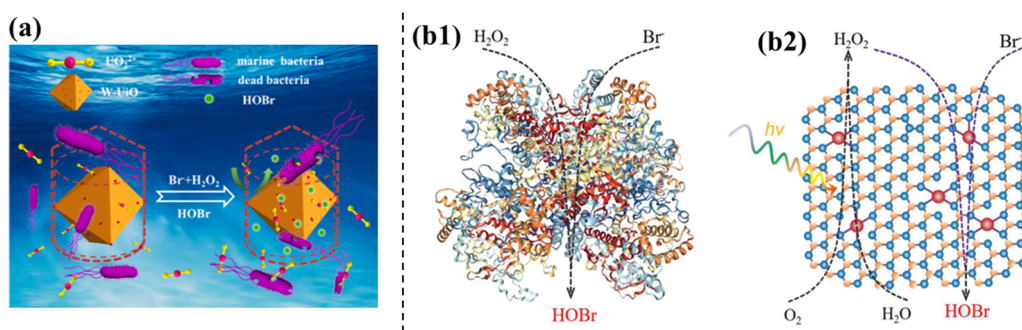


Fig. 7 (a) Schematic of the antibiofouling and uranium extraction process of W-UiO.<sup>69</sup> Reproduced from ref. 69 with permission from Elsevier, copyright 2022. (b) Schematic of the bifunctional Cr-SA-CN nanozyme: (b1) Bromide oxidation with H<sub>2</sub>O<sub>2</sub> on a natural vanadium bromoperoxidase, (b2) Schematic of the cascade reactions on an artificial bifunctional Cr-SA-CN nanozyme: photocatalytic H<sub>2</sub>O<sub>2</sub> production from water and O<sub>2</sub>, and *in situ* self-supply of H<sub>2</sub>O<sub>2</sub> for bromide oxidation reaction.<sup>70</sup> Reproduced from ref. 70 with permission from Wiley, copyright 2022.



Table 1 Summary of catalysts for oxidative halogenation reactions

Natural enzymes/ biomimetic enzymes	Dye [ $\times 10^{-6}$ M]	$\text{Br}^-$ [ $\times 10^{-3}$ M]	$\text{H}_2\text{O}_2$ [ $\times 10^{-3}$ M]	Catalyst [ $\times 10^6$ g mL $^{-1}$ ]	Reaction conditions	Ref.
V-HPO	50 <sup>a</sup>	100 <sup>c</sup>	2.50	—	—	72
$\text{V}_2\text{O}_5$	50 <sup>b</sup>	1	0.01	0–30	Tris- $\text{SO}_4$ buffer (0.1 M), pH = 8.3	17
$\text{CeO}_2$	50 <sup>a</sup>	25 <sup>c</sup>	0.30	25	23–25 °C	14
$\text{C}/\text{CeO}_2$	28 <sup>a</sup>	69.4 <sup>c</sup>	0.83	80	RT	20
N, C/ $\text{CeO}_2$	28 <sup>a</sup>	69.4 <sup>c</sup>	0.83	50	RT	21
Lan/ $\text{CeO}_2$	53.5 <sup>a</sup>	26.7 <sup>d</sup>	0.32	26.74	—	22
$\text{CeO}_2/\text{ZrO}_2$	50 <sup>a</sup>	25 <sup>c</sup>	0.35	50	25 °C	23
Ce-MOF-808	50 <sup>a</sup>	25 <sup>c</sup>	1	100	Acetate-acetic acid buffer, pH 5.5, 37 °C	51
Mo SA-N/C	50 <sup>a</sup>	25 <sup>c</sup>	0.80	100	Light-dependent	24
Co-MoS <sub>2</sub>	50 <sup>a</sup>	25 <sup>c</sup>	0.35	50	pH 5.7	25
W-Uio	50 <sup>a</sup>	25 <sup>c</sup>	0.49	50	pH 6	69
Cr-SA-CN	100 <sup>b</sup>	0.5	0.035	50	Tris- $\text{SO}_4$ buffer (0.1 M), pH = 8.1, dark	70

<sup>a</sup> PR. <sup>b</sup> MCD. <sup>c</sup>  $\text{NH}_4\text{Br}$ . <sup>d</sup> KBr. RT = room temperature.

## 6. Conclusion

In this review, we have summarized prevalent biomimetic haloperoxidases and briefly introduce their antifouling mechanism and effects. The oxidative halogenation reactions (several parameters, reaction conditions and catalytic activity) of different biomimetic catalysts were summarized and compared, as shown in Table 1. It can be observed that biomimetic catalysts have gone through many metal-based changes. Due to the toxicity of vanadium, the metallic groups changed from vanadium-based to cerium-based materials. In addition to cerium, there are also biomimetic haloperoxidases composed of molybdenum, cobalt, uranium, chromium and many more. Compared to other metal-based biomimetic haloperoxidases, ceria has a comparatively better catalytic performance. At the same substrate concentration, ceria requires less catalyst content. This is one reason why many catalysts are cerium-based. Another reason is that the catalytic reaction conditions containing ceria can be carried out at room temperature and do not depend on the limitations of pH or light.

Although several biomimetic haloperoxidases have been proposed and studied for antifouling applications, there is still a long way to go before biomimetic enzymes can truly replace natural enzymes. Biomimetic enzymes have overcome some of the shortcomings of natural enzymes, but their catalytic activity is still lower than that of natural enzymes. Moreover, they have a lower binding affinity. Since most biomimetic enzymes are nanozymes and many nanozymes have been shown to have the characteristics of multiplicate enzymes at the same time, it is not clear whether the activities of different enzymes will affect each other or not. Moreover, the antifouling mechanism of many biomimetic enzymes to kill the bacteria and inhibit the formation of biofilms has not been deeply explored, and the detailed mechanism needs to be further explored.

The catalytic activity of biomimetic enzymes can reach a higher level by effective optimization, such as size, morphology, composition and surface modification. Under the same cost conditions, the antifouling and antibacterial activities can be studied from a multi-functional point of view, and it may have a better effect than the single functional enzymes. There are

still many possibilities for the development of biomimetic enzymes in the field of antifouling in the future, such as exploring new, easily obtainable and environment-friendly metal biomimetic enzymes, modifying cerium oxides that has recently emerged to get better catalytic activity, combining biomimetic enzymes that prevent aggregation on the surface of biological cells and other classes of enzymes that inhibit growth or kill cells, and it can acquire a new biomimetic enzyme with better persistence and effectiveness. The development of modern society pays more attention to environmental friendliness and the safety and non-toxicity of the materials used, which is also in line with the advantages of biomimetic enzymes.

With the development of science and technology, researchers have explored various fields, which could promote the research on biomimetic enzyme antifouling in more detail. Researchers' enthusiastic exploration of biomimetic haloperoxidases and the rapid development of nanotechnology may solve existing problems of biofouling in the near future, and biomimetic haloperoxidases will flourish in the field of antifouling.

## Data availability

No primary research results, software or code have been included and no new data were generated or analyzed as part of this review.

## Conflicts of interest

The authors declare that they have no conflict of interest.

## Acknowledgements

The present work was supported by Shandong Provincial Natural Science Youth Fund Project (ZR2022QD001), National Natural Science Foundation of China (No. 42306228), Key R&D Program of Shandong Province, China (No. 2022CXPT027), Chinese



Academy of Sciences President's International Fellowship Initiative (No. 2023VEA0007) and the Taishan Scholars Program.

## References

- N. Høiby, *J. Pathol. Microbiol. Immunol.*, 2017, **125**, 272–275.
- Y. A. Nikolaev and V. K. Plakunov, *Microbiology*, 2007, **76**, 125–138.
- M. S. Rahaman, H. Thérien-Aubin, M. Ben-Sasson, C. K. Ober, M. Nielsen and M. Elimelech, *J. Mater. Chem. B*, 2014, **2**, 1724–1732.
- M. H. Mohd, M. A. Zalaya, M. Latheef, H. S. Choi, M. A. A. Rahman and D. K. Kim, *Lat. Am. J. Solids Struct.*, 2019, **16**, e182.
- M. E. Callow and J. A. Callow, *Biologist*, 2002, **49**, 1–5.
- M. Salta, J. A. Wharton, P. Stoodley, S. P. Dennington, L. R. Goodes, S. Werwinski, U. Mart, R. J. K. Wood and K. R. Stokes, *Philos. Trans. R. Soc., A*, 2010, **368**, 4729–4754.
- S. K. Chakraborty, in *Impacts of Invasive Species on Coastal Environments: Coasts in Crisis*, ed. C. Makowski and C. W. Finkl, Springer International Publishing, Cham, 2019, pp. 171–245, DOI: [10.1007/978-3-319-91382-7\\_6](https://doi.org/10.1007/978-3-319-91382-7_6).
- L. Chen, Y. Duan, M. Cui, R. Huang, R. Su, W. Qi and Z. He, *Sci. Total Environ.*, 2021, **766**, 144469.
- K. Bosselmann, in *Tributyltin: Case Study of an Environmental Contaminant*, ed. S. J. De Mora, Cambridge University Press, Cambridge, 1996, pp. 237–263, DOI: [10.1017/CBO9780511759772.009](https://doi.org/10.1017/CBO9780511759772.009).
- S. Sonak, P. Pangam, A. Giriyam and K. Hawaldar, *J. Environ. Manage.*, 2009, **90**, S96–S108.
- H. Jin, L. Tian, W. Bing, J. Zhao and L. Ren, *Prog. Mater. Sci.*, 2022, **124**, 100889.
- I. Banerjee, R. C. Pangule and R. S. Kane, *Adv. Mater.*, 2011, **23**, 690–718.
- J. R. Almeida and V. Vasconcelos, *Biotechnol. Adv.*, 2015, **33**, 343–357.
- K. Herget, P. Hubach, S. Pusch, P. Deglmann, H. Götz, T. E. Gorelik, I. Y. A. Gural'skiy, F. Pfitzner, T. Link, S. Schenk, M. Panthöfer, V. Ksenofontov, U. Kolb, T. Opatz, R. André and W. Tremel, *Adv. Mater.*, 2017, **29**, 1603823.
- A. Butler and M. Sandy, *Nature*, 2009, **460**, 848–854.
- R. I. De la Rosa, M. J. Clague and A. Butler, *J. Am. Chem. Soc.*, 1992, **114**, 760–761.
- F. Natalio, R. André, A. F. Hartog, B. Stoll, K. P. Jochum, R. Wever and W. Tremel, *Nat. Nanotechnol.*, 2012, **7**, 530–535.
- G. J. Colpas, B. J. Hamstra, J. W. Kampf and V. L. Pecoraro, *J. Am. Chem. Soc.*, 1996, **118**, 3469–3478.
- R. Wu, W. Wang, Q. Luo, X. Zeng, J. Li, Y. Li, Y. Li, J. Li and N. Wang, *Adv. Compos. Hybrid Mater.*, 2022, **5**, 2163–2170.
- N. Wang, W. Q. Li, Y. D. Ren, J. Z. Duan, X. F. Zhai, F. Guan, L. F. Wang and B. R. Hou, *Colloids Surf., A*, 2020, **608**, 125592.
- N. Wang, X. F. Zhai, F. Guan, R. Y. Zhang, B. R. Hou and J. Z. Duan, *Int. J. Mol. Sci.*, 2023, **24**.
- P. Opitz, O. Jegel, J. Nasir, T. Rios-Studer, A. Gazanis, D.-H. Pham, K. Domke, R. Heermann, J. Schmedt auf der Gunne and W. Tremel, *Nanoscale*, 2022, **14**, 4740–4752.
- Q. Luo, Y. Li, X. Huo, J. Li, L. Li, W. Wang, Y. Li, S. Chen, Y. Song and N. Wang, *Small*, 2022, **18**, e2107401.
- W. Wang, Q. Luo, J. Li, L. Li, Y. Li, X. Huo, X. Du, Z. Li and N. Wang, *Adv. Funct. Mater.*, 2022, **32**, 2205461.
- Q. Luo, J. Li, W. Wang, Y. Li, Y. Li, X. Huo, J. Li and N. Wang, *ACS Appl. Mater. Interfaces*, 2022, **14**, 14218–14225.
- Y. Tao, E. Ju, J. Ren and X. Qu, *Adv. Mater.*, 2015, **27**, 1097–1104.
- G. Fang, W. Li, X. Shen, J. M. Perez-Aguilar, Y. Chong, X. Gao, Z. Chai, C. Chen, C. Ge and R. Zhou, *Nat. Commun.*, 2018, **9**, 129.
- Z. Hasan, R. Renirie, R. Kerkman, H. J. Ruijssenaars, A. F. Hartog and R. Wever, *J. Biol. Chem.*, 2006, **281**, 9738–9744.
- Z. Chen, *Coord. Chem. Rev.*, 2022, **457**, 214404.
- M. J. Clague, N. L. Keder and A. Butler, *Inorg. Chem.*, 1993, **32**, 4754–4761.
- E. Palmajumder, S. Patra, M. G. B. Drew and K. K. Mukherjea, *New J. Chem.*, 2016, **40**, 8696–8703.
- M. R. Maurya, N. Chaudhary and F. Avecilla, *Polyhedron*, 2014, **67**, 436–448.
- R. André, F. Natália, M. Humanes, J. Leppin, K. Heinze, R. Wever, H.-C. Schröder, W. E. G. Müller and W. Tremel, *Adv. Funct. Mater.*, 2011, **21**, 501–509.
- I. Paterson, *Science*, 2005, **310**, 451–453.
- J. Asakura and M. J. Robins, *J. Org. Chem.*, 1990, **55**, 4928–4933.
- A. Leyva-Pérez, D. Cóbita-Merchán, J. R. Cabrero-Antonino, S. I. Al-Resayes and A. Corma, *ACS Catal.*, 2013, **3**, 250–258.
- R. J. Field, E. Koros and R. M. Noyes, *J. Am. Chem. Soc.*, 1972, **94**, 8649–8664.
- C. T. Campbell and C. H. F. Peden, *Science*, 2005, **309**, 713–714.
- S. Deshpande, S. Patil, S. V. Kuchibhatla and S. Seal, *Appl. Phys. Lett.*, 2005, **87**, 133113.
- G. S. Herman, *Surf. Sci.*, 1999, **437**, 207–214.
- E. Pütz, G. J. Smales, O. Jegel, F. Emmerling and W. Tremel, *Nanoscale*, 2022, **14**, 13639–13650.
- T. R. Garrett, M. Bhakoo and Z. Zhang, *Prog. Natl. Sci.*, 2008, **18**, 1049–1056.
- M. Hu, K. Korschelt, M. Viel, N. Wiesmann, M. Kappl, J. Brieger, K. Landfester, H. Thérien-Aubin and W. Tremel, *ACS Appl. Mater. Interfaces*, 2018, **10**, 44722–44730.
- C. Xie, Y. Ma, P. Zhang, J. Zhang, X. Li, K. Zheng, A. Li, W. Wu, Q. Pang, X. He and Z. Zhang, *Environ. Sci.: Nano*, 2021, **8**, 1701–1712.
- H. An, L. Liu, N. Song, H. Zhu and Y. Tang, *Nano Res.*, 2023, **16**, 3622–3640.
- H. Wei and E. Wang, *Chem. Soc. Rev.*, 2013, **42**, 6060–6093.
- Z. Ji, X. Wang, H. Zhang, S. Lin, H. Meng, B. Sun, S. George, T. Xia, A. E. Nel and J. I. Zink, *ACS Nano*, 2012, **6**, 5366–5380.
- R. Schmitt, A. Nenning, O. Kraynis, R. Korobko, A. I. Frenkel, I. Lubomirsky, S. M. Haile and J. L. M. Rupp, *Chem. Soc. Rev.*, 2020, **49**, 554–592.



49 V. Šepelák, A. Düvel, M. Wilkening, K.-D. Becker and P. Heitjans, *Chem. Soc. Rev.*, 2013, **42**, 7507–7520.

50 B. Weng, K.-Q. Lu, Z. Tang, H. M. Chen and Y.-J. Xu, *Nat. Commun.*, 2018, **9**, 1543.

51 Z. Zhou, S. Li, G. Wei, W. Liu, Y. Zhang, C. Zhu, S. Liu, T. Li and H. Wei, *Adv. Funct. Mater.*, 2022, **32**, 2206294.

52 L. Ma, F. Jiang, X. Fan, L. Wang, C. He, M. Zhou, S. Li, H. Luo, C. Cheng and L. Qiu, *Adv. Mater.*, 2020, **32**, 2003065.

53 H. Furukawa, K. E. Cordova, M. O'Keeffe and O. M. Yaghi, *Science*, 2013, **341**, 1230444.

54 A. H. Chughtai, N. Ahmad, H. A. Younus, A. Laypkov and F. Verpoort, *Chem. Soc. Rev.*, 2015, **44**, 6804–6849.

55 J. Wu, Z. Wang, X. Jin, S. Zhang, T. Li, Y. Zhang, H. Xing, Y. Yu, H. Zhang, X. Gao and H. Wei, *Adv. Mater.*, 2021, **33**, 2005024.

56 M. Li, J. Chen, W. Wu, Y. Fang and S. Dong, *J. Am. Chem. Soc.*, 2020, **142**, 15569–15574.

57 H. Wei, L. Gao, K. Fan, J. Liu, J. He, X. Qu, S. Dong, E. Wang and X. Yan, *Nano Today*, 2021, **40**, 101269.

58 W. Wu, L. Huang, E. Wang and S. Dong, *Chem. Sci.*, 2020, **11**, 9741–9756.

59 L. Jiao, H. Y. Yan, Y. Wu, W. L. Gu, C. Z. Zhu, D. Du and Y. H. Lin, *Angew. Chem., Int. Ed.*, 2020, **59**, 2565–2576.

60 B. L. Xu, H. Wang, W. W. Wang, L. Z. Gao, S. S. Li, X. T. Pan, H. Y. Wang, H. L. Yang, X. Q. Meng, Q. W. Wu, L. R. Zheng, S. M. Chen, X. H. Shi, K. L. Fan, X. Y. Yan and H. Y. Liu, *Angew. Chem., Int. Ed.*, 2019, **58**, 4911–4916.

61 X. Wang, Q. Shi, Z. Zha, D. Zhu, L. Zheng, L. Shi, X. Wei, L. Lian, K. Wu and L. Cheng, *Bioact. Mater.*, 2021, **6**, 4389–4401.

62 E. L. K. Chng, Z. Sofer and M. Pumera, *Nanoscale*, 2014, **6**, 14412–14418.

63 S. Arefi-Oskoui, A. Khataee, O. K. Ucun, M. Koby, T. O. Hancı and I. Arslan-Alaton, *Chemosphere*, 2021, **268**, 128822.

64 W. Liu, X. Dai, Z. Bai, Y. Wang, Z. Yang, L. Zhang, L. Xu, L. Chen, Y. Li, D. Gui, J. Diwu, J. Wang, R. Zhou, Z. Chai and S. Wang, *Environ. Sci. Technol.*, 2017, **51**, 3911–3921.

65 W. Luo, G. Xiao, F. Tian, J. J. Richardson, Y. Wang, J. Zhou, J. Guo, X. Liao and B. Shi, *Energy Environ. Sci.*, 2019, **12**, 607–614.

66 H. Zhou, M. Zheng, H. Tang, B. Xu, Y. Tang and H. Pang, *Small*, 2020, **16**, 1904252.

67 Y. Bai, C. Liu, Y. Shan, T. Chen, Y. Zhao, C. Yu and H. Pang, *Adv. Energy Mater.*, 2022, **12**, 2100346.

68 Z. Huang, H. Dong, N. Yang, H. Li, N. He, X. Lu, J. Wen and X. Wang, *ACS Appl. Mater. Interfaces*, 2020, **12**, 16959–16968.

69 W. Wang, Q. Luo, J. Li, Y. Li, R. Wu, Y. Li, X. Huo and N. Wang, *Chem. Eng. J.*, 2022, **431**, 133483.

70 Q. Luo, Y. Li, X. Huo, L. Li, Y. Song, S. Chen, H. Lin and N. Wang, *Adv. Sci.*, 2022, **9**, e2105346.

71 L.-S. Zhang and G. T. F. Wong, *Talanta*, 1999, **48**, 1031–1038.

72 B. Sels, D. D. Vos, M. Buntinx, F. Pierard, A. Kirsch-De Mesmaeker and P. Jacobs, *Nature*, 1999, **400**, 855–857.

